The Journal of Chemical Physics

Quasi-analytical resolution-correction of elastic neutron scattering from proteins

Cite as: J. Chem. Phys. **157**, 134103 (2022); https://doi.org/10.1063/5.0103960
Submitted: 17 June 2022 • Accepted: 07 September 2022 • Accepted Manuscript Online: 07 September 2022 • Published Online: 05 October 2022

Abir N. Hassani, Andreas M. Stadler and Gerald R. Kneller

View Online Export Citation CrossMark

ARTICLES YOU MAY BE INTERESTED IN

Multiscale relaxation dynamics and diffusion of myelin basic protein in solution studied by quasielastic neutron scattering
The Journal of Chemical Physics **156**, 025102 (2022); https://doi.org/10.1063/5.0077100

Relating dynamic free volume to cooperative relaxation in a glass-forming polymer composite
The Journal of Chemical Physics **157**, 131101 (2022); https://doi.org/10.1063/5.0114902

Communication: Electronic transition of the l-C_6^+ cation at 417 nm
The Journal of Chemical Physics **157**, 121102 (2022); https://doi.org/10.1063/5.0106183

Webinar
Meet the Lock-in Amplifiers that measure microwaves
Oct. 6th – Register now
Zurich Instruments

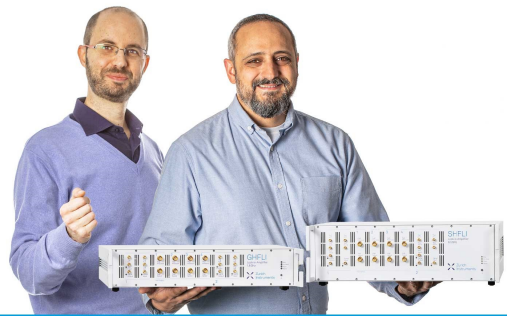

© 2022 Author(s).

The Journal of Chemical Physics ARTICLE scitation.org/journal/jcp

Quasi-analytical resolution-correction of elastic neutron scattering from proteins

Cite as: J. Chem. Phys. **157**, 134103 (2022); doi: 10.1063/5.0103960
Submitted: 17 June 2022 • Accepted: 7 September 2022 •
Published Online: 5 October 2022

View Online Export Citation CrossMark

Abir N. Hassani,[1,2,3] Andreas M. Stadler,[3,4,a)] and Gerald R. Kneller[1,2,b)]

AFFILIATIONS

[1] Centre de Biophysique Moléculaire, CNRS and Univ. d'Orléans, Rue Charles Sadron, 45071 Orléans, France
[2] Synchrotron Soleil, L'Orme de Merisiers, 91192 Gif-sur-Yvette, France
[3] Jülich Centre for Neutron Science (JCNS-1) and Institute of Biological Information Processing (IBI-8), Forschungszentrum Jülich GmbH, 52425 Jülich, Germany
[4] Institute of Physical Chemistry, RWTH Aachen University, Landoltweg 2, 52056 Aachen, Germany

[a)] **E-mail:** a.stadler@fz-juelich.de
[b)] **Author to whom correspondence should be addressed:** gerald.kneller@cnrs.fr

ABSTRACT

Elastic neutron scattering from proteins reflects the motional amplitudes resulting from their internal collective and single-atom dynamics and is observable if the global diffusion of whole molecules is either blocked or cannot be resolved by the spectrometer under consideration. Due to finite instrumental resolution, the measured elastic scattering amplitude always contains contaminations from quasielastic neutron scattering and some model must be assumed to extract the resolution-corrected counterpart from corresponding experimental spectra. Here, we derive a quasi-analytical method for that purpose, assuming that the intermediate scattering function relaxes with a "stretched" Mittag-Leffler function, $E_\alpha(-(t/\tau)^\alpha)$ $(0 < \alpha < 1)$, toward the elastic amplitude and that the instrumental resolution function has Gaussian form. The corresponding function can be integrated into a fitting procedure and allows for eliminating the elastic intensity as a fit parameter. We illustrate the method for the analysis of two proteins in solution, the intrinsically disordered Myelin Basic Protein, confirming recently published results [Hassani *et al.*, J. Chem. Phys. **156**, 025102 (2022)], and the well-folded globular protein myoglobin. We also briefly discuss the consequences of our findings for the extraction of mean square position fluctuations from elastic scans.

Published under an exclusive license by AIP Publishing. https://doi.org/10.1063/5.0103960

I. INTRODUCTION

Thermal neutron scattering is a powerful and versatile spectroscopic method to probe the structural dynamics of condensed matter systems.[1] An important application concerns quasielastic neutron scattering (QENS) from proteins, which gives information about the diffusion and the relaxation dynamics of these macromolecules.[2–6] To probe the internal non-exponential multiscale relaxation dynamics, which is crucial for their function and typical for complex systems, in general,[7–10] one can either use hydrated powder samples, where global diffusional motions are simply blocked, or probe a protein solution with a spectrometer that will not resolve these motions. In both cases, information about the motional amplitudes of internal protein dynamics is contained in the elastic amplitude and elastic scans are thus, in principle, sufficient to obtain this information. One must, however, be aware that the extracted motional amplitudes are underestimated due to the unavoidable contamination of the elastic amplitude by contributions from quasielastic scattering, and this correction can be particularly important for slowly relaxing systems.[11] Noting that the "true" elastic amplitude defines the asymptotic form of the neutron intermediate scattering function at infinite time, it can only be obtained by assuming some model for that function. A corresponding "minimalistic" model has been recently proposed and motivated in Ref. 12 and was then applied in a few subsequent QENS studies of protein dynamics,[13–15] as well as for confined water molecules in clays.[16] In all these studies the elastic amplitude was a fit parameter, which left some ambiguity about the physical significance of the resulting fits, in particular, since fit parameters are quite interdependent. The goal of this paper is to replace the elastic intensity as a fit parameter by an estimation on the basis of its experimentally measured counterpart, the assumed model for the relaxation function, and the resolution of the instrument under consideration. Computational efficiency is here a fundamental aspect since it enables the integration of the corresponding function into

Published under an exclusive license by AIP Publishing

the fitting procedure for the remaining parameters of the relaxation function.

This paper is organized as follows: The core of the paper is contained in Secs. II and III, which describe the theoretical background and the method, followed by Sec. IV showing some applications, and the conclusions in Sec. V.

II. THEORETICAL BACKGROUND

A. Scattering functions

In standard neutron scattering experiments one measures the dynamic structure factor,

$$\tilde{F}(\mathbf{q},\omega) = \frac{1}{2\pi}\int_{-\infty}^{+\infty} dt\, e^{-i\omega t} F(\mathbf{q},t), \tag{1}$$

which is the time Fourier transform of the intermediate scattering function containing the information about the structural dynamics of the system under consideration,

$$F(\mathbf{q},t) = \frac{1}{N}\sum_{j,k}\Gamma_{jk}\left\langle e^{-i\mathbf{q}\cdot\hat{\mathbf{R}}_j(0)} e^{i\mathbf{q}\cdot\hat{\mathbf{R}}_k(t)}\right\rangle. \tag{2}$$

Usually, the dynamic structure factor is denoted by $S(\mathbf{q},\omega)$, but we use the symbol $\tilde{F}(\mathbf{q},\omega)$ to label Fourier transforms in a uniform way. The scattering-related quantities are, respectively, the momentum and energy transfer from the neutron to the sample, $\mathbf{q}$ and ω, in units of $\hbar$, N is the total number of atoms in the scattering system and for each pair $\{j,k\}$ of them, $\{\hat{\mathbf{R}}_j(t), \hat{\mathbf{R}}_k(t)\}$ denote the associated time-dependent position operators. The symbol $\langle\cdots\rangle$ stands for a quantum ensemble average and the weighting factors Γ_{jk} have the form

$$\Gamma_{jk} = \overline{b_j}^{\,*}\,\overline{b_k} + \delta_{jk}\overline{|b_j - \overline{b_j}|^2}, \tag{3}$$

where b_j and b_k are the (complex) scattering lengths[1,17] of the atoms j and k, respectively. For a given atom, the average runs over all isotopes and combinations of the nuclear and neutron spins and we note that $b_{j,\mathrm{coh}} \equiv \overline{b_j}$ and $b_{j,\mathrm{inc}} \equiv (\overline{|b_j - \overline{b_j}|^2})^{1/2}$ are, respectively, the coherent and incoherent scattering lengths of atom j. Coherent and incoherent scattering probe, respectively, the collective and average single atom dynamics of the system under consideration, but since these scattering types are not separable without special spin-polarization experiments,[18–20] we will not explicitly distinguish between them.

The intermediate scattering function fulfills the symmetry relations of a quantum time correlation function,

$$F^*(\mathbf{q},t) = F(\mathbf{q},-t), \tag{4}$$

$$F(\mathbf{q},-t) = F(-\mathbf{q},t+i\beta\hbar), \tag{5}$$

where $\beta = 1/k_B T$ is the inverse Boltzmann temperature. For the dynamic structure factor, Eq. (5) translates into

$$\tilde{F}(\mathbf{q},\omega) = e^{\beta\hbar\omega}\tilde{F}(-\mathbf{q},-\omega), \tag{6}$$

which is the well-known detailed-balance relation.

B. Elastic and inelastic scattering

Noting that

$$e^{i\mathbf{q}\cdot\hat{\mathbf{R}}_j(t)} = \int d^3r\, \exp(-i\mathbf{q}\cdot\mathbf{r})\delta(\mathbf{r} - \hat{\mathbf{R}}_j(t))$$

is the spatially Fourier-transformed single particle density for atom j, we introduce the deviation of this quantity with respect to its mean value,

$$\delta\tilde{\alpha}_k(\mathbf{q},t) = e^{i\mathbf{q}\cdot\hat{\mathbf{R}}_j(t)} - \left\langle e^{i\mathbf{q}\cdot\hat{\mathbf{R}}_j(t)}\right\rangle, \tag{7}$$

to split the intermediate scattering function into a static and a time-dependent component,

$$F(\mathbf{q},t) = F(\mathbf{q},\infty) + \delta F(\mathbf{q},t), \tag{8}$$

which are given by

$$F(\mathbf{q},\infty) = \frac{1}{N}\sum_{j,k}\Gamma_{jk}\left\langle e^{i\mathbf{q}\cdot\hat{\mathbf{R}}_j}\right\rangle^*\left\langle e^{i\mathbf{q}\cdot\hat{\mathbf{R}}_k}\right\rangle, \tag{9}$$

$$\delta F(\mathbf{q},t) = \frac{1}{N}\sum_{j,k}\Gamma_{jk}\left\langle \delta\tilde{\alpha}_j^\dagger(\mathbf{q},0)\delta\tilde{\alpha}_k(\mathbf{q},t)\right\rangle. \tag{10}$$

Making the physically reasonable assumption

$$\lim_{t\to\infty}\delta F(\mathbf{q},t) = 0 \tag{11}$$

shows that $F(\mathbf{q},\infty)$ is the asymptotic form of the intermediate scattering function and it follows by the Fourier transform of Eq. (8) that

$$\tilde{F}(\mathbf{q},\omega) = F(\mathbf{q},\infty)\delta(\omega) + \delta\tilde{F}(\mathbf{q},\omega). \tag{12}$$

Therefore, $F(\mathbf{q},\infty)$ represents the elastic amplitude of the Fourier spectrum and $\delta\tilde{F}(\mathbf{q},\omega)$ its inelastic component. Here, "inelastic" is to be understood as "non-elastic" and includes also the quasielastic component of the spectrum, which is very close to the elastic line and describes relaxation and diffusion processes.

C. Generic form of the scattering functions

For modeling purposes, it is convenient to introduce the normalized relaxation function

$$\phi(\mathbf{q},t) = \delta F(\mathbf{q},t)/\delta F(\mathbf{q},0), \tag{13}$$

noting that this function does not monotonously decay for short times. This leads to the generic form

$$F(\mathbf{q},t) = F(\mathbf{q},\infty) + (F(\mathbf{q},0) - F(\mathbf{q},\infty))\phi(\mathbf{q},t) \tag{14}$$

of the intermediate scattering function, which translates into the corresponding generic form

$$\tilde{F}(\mathbf{q},\omega) = F(\mathbf{q},\infty)\delta(\omega) + (F(\mathbf{q},0) - F(\mathbf{q},\infty))\tilde{\phi}(\mathbf{q},\omega), \tag{15}$$

of the dynamic structure factor. We note that

$$F(\mathbf{q},0) = \frac{1}{N}\sum_{j,k}\Gamma_{jk}\left\langle e^{i\mathbf{q}\cdot(\hat{\mathbf{R}}_k - \hat{\mathbf{R}}_j)}\right\rangle \tag{16}$$

Published under an exclusive license by AIP Publishing

is the total static structure factor, which tends for $q \equiv |\mathbf{q}| \to \infty$ to a constant value,

$$\lim_{q\to\infty} F(\mathbf{q},0) = \frac{1}{N}\sum_k \Gamma_{kk}, \tag{17}$$

and oscillates for smaller q-values around that constant. For modeling purposes, it is convenient to normalize the intermediate scattering function such that

$$\frac{1}{N}\sum_k \Gamma_{kk} = 1. \tag{18}$$

D. Hydrogen-rich systems

We finally consider the frequent of case of neutron scattering from hydrogen-rich systems, such as proteins and polymers. Because of the exceptionally large cross section for incoherent scattering from hydrogen, it is sufficient to consider only these atoms, setting $\Gamma_{jk} = \delta_{jk}$. With the normalization (18) it then follows that

$$F(\mathbf{q},0) = 1, \tag{19}$$

and the generic form of the intermediate scattering function simplifies to

$$F(\mathbf{q},t) = EISF(\mathbf{q}) + (1 - EISF(\mathbf{q}))\phi(\mathbf{q},t), \tag{20}$$

where

$$EISF(\mathbf{q}) = \frac{1}{N}\sum_{j\in\mathbb{H}} \left| \left\langle e^{i\mathbf{q}\cdot\hat{\mathbf{R}}_j} \right\rangle \right|^2 \tag{21}$$

is referred to as elastic incoherent structure factor and the relaxation function has the form

$$\phi(\mathbf{q},t) = \frac{\sum_{j\in\mathbb{H}} \left\langle \delta\tilde{\alpha}_j^\dagger(\mathbf{q},0)\delta\tilde{\alpha}_j(\mathbf{q},t) \right\rangle}{\sum_{j\in\mathbb{H}} \left\langle \delta\tilde{\alpha}_j^\dagger(\mathbf{q},0)\delta\tilde{\alpha}_j(\mathbf{q},0) \right\rangle}. \tag{22}$$

III. PSEUDOELASTIC SCATTERING

A. Measured and true elastic intensity

We will now consider a measured dynamic structure factor, which is always broadened due to finite instrumental resolution. Defining $\tilde{R}(\omega)$ to be the instrumental resolution function and omitting for simplicity the q-dependence of the relevant quantities, the measured dynamic structure factor is given by the frequency convolution of the true dynamic structure factor and the resolution function,

$$\tilde{F}_m(\omega) = (\tilde{R} * \tilde{F})(\omega) \equiv \int_{-\infty}^{+\infty} d\omega'\, \tilde{R}(\omega-\omega')\tilde{F}(\omega'). \tag{23}$$

With (15), we obtain then in a first step

$$\tilde{F}_m(\omega) = F(\infty)\tilde{R}(\omega) + (F(0) - F(\infty))(\tilde{R} * \tilde{\phi})(\omega). \tag{24}$$

We define now the measured elastic intensity through the integral

$$F_m(\infty) \equiv \int_{-\epsilon}^{+\epsilon} d\omega\, \tilde{F}_m(\omega), \tag{25}$$

where $\epsilon > 0$ is defined such that

$$\int_{-\epsilon}^{+\epsilon} d\omega\, \tilde{R}(\omega) \lessapprox 1, \tag{26}$$

and the measured total static structure factor through

$$F_m(0) \equiv \int_{\omega_{\min}}^{\omega_{\max}} d\omega\, \tilde{F}_m(\omega), \tag{27}$$

where $[\omega_{\min}, \omega_{\max}]$ is the dynamical range of the instrument. It follows then from the generic form (24) of the measured, resolution-broadened dynamic structure factor that

$$F_m(\infty) \approx F(\infty) + (F_m(0) - F(\infty))\xi, \tag{28}$$

where ξ is the pseudoelastic contribution due to finite instrumental resolution,

$$\xi = \int_{-\epsilon}^{+\epsilon} d\omega\, (\tilde{R} * \tilde{\phi})(\omega). \tag{29}$$

Supposing that this contribution can be reliably computed on the basis of appropriate models for the relaxation function and the instrumental resolution, the "true" elastic intensity may be estimated through

$$F(\infty) \approx \frac{F_m(\infty) - \xi F_m(0)}{1-\xi}. \tag{30}$$

For essentially incoherent scattering, the measured total structure factor is not needed, since one knows that the incoherent static structure factor is simply a constant. Assuming the normalization (18), one can replace $F_m(0) \to 1$ in this case. It is also worthwhile noting that the standard definition of the elastic amplitude[21,22] corresponds in our notation to the measured one.

B. Model

1. Symmetrized correlation function

The symmetry relations (4) and (5) show that the intermediate scattering function becomes a real symmetrical function in time if one considers the classical limit $\hbar \to 0$ and if one can assume that the scattering functions are invariant with respect to the parity operation $\mathbf{q} \to -\mathbf{q}$. Based on this observation, Schofield proposed to use the time-symmetrized real function $F^{(+)}(\mathbf{q},t) \equiv F(\mathbf{q}, t + i\beta\hbar/2)$ to define the semiclassical approximation $F^{(+)}(\mathbf{q},t) \approx F^{(cl)}(\mathbf{q},t)$.[23] To be able to work with classical relaxation models, we consider now the time-symmetrized generic form

$$F^{(+)}(t) = F(\infty) + (F(0) - F(\infty))\phi^{(+)}(t) \tag{31}$$

of the intermediate scattering function, where the relaxation function is defined as

$$\phi^{(+)}(t) \equiv \frac{\phi(t + i\beta\hbar/2)}{\phi(i\beta\hbar/2)}, \tag{32}$$

in order to ensure its correct normalization.

Published under an exclusive license by AIP Publishing

2. "Minimalistic" model

We assume now that the symmetrized relaxation function is well represented by the model

$$\phi^{(+)}(t) = \phi_{\mathrm{ML}}(t), \tag{33}$$

where $\phi_{\mathrm{ML}}(\cdot)$ is the "stretched" Mittag-Leffler (ML) function,

$$\phi_{\mathrm{ML}}(t) \equiv E_\alpha(-(|t|/\tau)^\alpha) \quad (0 < \alpha \leq 1). \tag{34}$$

The Mittag-Leffler function, $E_\alpha(z)$, is an entire function in the complex plane,[24] and the Taylor series $E_\alpha(z) = \sum_{n=0}^{\infty} \frac{z^n}{\Gamma(1+\alpha n)}$ shows that $E_1(z) = \exp(z)$. The most important property of the model relaxation function (34) is that it decays asymptotically with a power law,

$$\phi_{\mathrm{ML}}(t) \overset{t\to\infty}{\sim} \frac{(t/\tau)^{-\alpha}}{\Gamma(1-\alpha)}. \tag{35}$$

Inserting (34) into the generic form (31) of the symmetrized intermediate scattering leads to the model

$$F^{(+)}(t) = F(\infty) + (F(0) - F(\infty))E_\alpha(-(|t|/\tau)^\alpha), \tag{36}$$

which has *a priori* three parameters:

1. the time scale parameter, τ,
2. the form parameter, α, and
3. the plateau value $F(\infty) \equiv \lim_{t\to\infty} F^{(+)}(t)$.

In this form the model has been used in recent publications,[13–15] noting that only incoherent scattering has been considered, where $F(0) = 1$. In the following this restriction will not be made, assuming that an estimation for $F(0) \equiv F(\mathbf{q}, 0)$ can be provided according to Eq. (27).

The dynamic structure factor corresponding to the model (36) has then the form

$$S^{(+)}(\omega) = F(\infty)\delta(\omega) + (F(0) - F(\infty))\tilde{\phi}_{\mathrm{ML}}(\omega), \tag{37}$$

where the Fourier transformed relaxation function is a "generalized Lorentzian,"[25]

$$\tilde{\phi}_{\mathrm{ML}}(\omega) = \frac{\sin\left(\frac{\pi\alpha}{2}\right)}{\pi\omega\left((\tau\omega)^{-\alpha} + (\tau\omega)^\alpha + 2\cos\left(\frac{\pi\alpha}{2}\right)\right)}, \tag{38}$$

which follows from the even simpler analytical form of its Laplace transform,[24]

$$\hat{\phi}_{\mathrm{ML}}(s) = \frac{1}{s(1 + (s\tau)^{-\alpha})}, \tag{39}$$

by using the identity $\tilde{\phi}_{\mathrm{ML}}(\omega) = \Re\{\hat{\phi}_{\mathrm{ML}}(i\omega)\}$. The Fourier spectrum (38) becomes a "normal" Lorentzian function for $\alpha \to 1$.

3. Choice of the model

The ML relaxation function has the remarkable property of being close to self-similar ("weakly self-similar")[26] for every $t > 0$ and the physical reason for using it as model relaxation function are developed in Ref. 27. We resume here the essential points. From a mathematical point of view the ML relaxation verifies a fractional differential equation of the form[24,28]

$$\partial_t \phi_{\mathrm{ML}}(t) + \tau^{-\alpha} \underbrace{\frac{d}{dt}\int_0^t dt' \frac{(t-t')^{\alpha-1}}{\Gamma(\alpha)}\phi_{\mathrm{ML}}(t')}_{\partial_t^{1-\alpha}\phi_{\mathrm{ML}}(t)} = 0, \tag{40}$$

where $\partial_t^{1-\alpha}$ denotes a fractional derivative[29] of order $1-\alpha$. From a physical point of view Eq. (40) can be considered as a special form of the general equation of motion,

$$\partial_t \phi^{(+)}(t) + \int_0^t dt' \kappa^{(+)}(t-t')\phi^{(+)}(t') = 0, \tag{41}$$

that any symmetric time correlation function fulfills according to the Mori–Zwanzig theory of the Generalized Langevin equation.[30–32] Here, $\kappa^{(+)}(t)$ is the associated memory kernel, which is itself a time autocorrelation function that can be formally derived from the Hamiltonian of the dynamical system under consideration. The only point that matters here is to consider that the memory kernel has essentially two characteristic time scales, τ and τ^*, where τ characterizes the asymptotic regime of the correlation function $\phi^{(+)}(t)$ and τ^* the transition to that regime. In Ref. 27, it is then shown that the ML relaxation function emerges whenever $\tau^* \ll \tau$. Writing $\kappa^{(+)}(t) \equiv \kappa^{(+)}(t;\, \tau, \tau^*)$, we have then

$$\phi^{(+)}(t;\tau,\tau^*) \overset{\tau^*\to 0}{\sim} \phi_{\mathrm{ML}}^{(+)}(t), \tag{42}$$

and the fractional derivative in Eq. (40) thus represents the asymptotic form of a memory kernel.

4. Pseudoelastic model contribution

The estimation of the plateau value of a function from experimental data with an instrument-limited finite time range is clearly a delicate task and it is desirable to be to have some consistency check in which experimental data are used. This can be achieved if the pseudoelastic contribution, ξ, can be efficiently corrected for the given model relaxation function, such that the estimation (30) can be integrated into the fitting procedure. For this purpose, we will assume that the resolution function is well represented by a Gaussian function,

$$\tilde{R}(\omega) = \frac{1}{\sqrt{2\pi}\sigma} e^{-\frac{\omega^2}{2\sigma^2}} \longleftrightarrow R(t) = e^{-\frac{\sigma^2 t^2}{2}}, \tag{43}$$

where σ is approximately the half width at half maximum (HWHM) of the instrument under consideration. Working with symmetrized neutron scattering spectra and the model relaxation function $\phi_{\mathrm{ML}}(t)$, the resulting pseudoelastic contribution becomes then a function of the parameters α, τ, and σ,

$$\xi_{\mathrm{ML}}(\tau,\alpha,\sigma) = \int_{-\epsilon}^{+\epsilon} d\omega\, (\tilde{R} * \tilde{\phi}_{\mathrm{ML}})(\omega), \tag{44}$$

such that

$$F(\infty;\tau,\alpha,\sigma) \approx \frac{F_m(\infty) - \xi_{\mathrm{ML}}(\tau,\alpha,\sigma)F_m(0)}{1 - \xi_{\mathrm{ML}}(\tau,\alpha,\sigma)} \tag{45}$$

replaces the fit parameter $F(\infty)$. For a Gaussian function, we have $\int_{-3\sigma}^{+3\sigma} d\omega\, \tilde{R}(\omega) \approx 0.9978$ such that $\epsilon = 3\sigma$ is a good choice.

Published under an exclusive license by AIP Publishing

C. Computing ξ_{ML}

In order to obtain a quasi-analytical formula for the pseudoelastic contribution ξ_{ML} defined in Eq. (44), we introduce the boxcar function

$$\tilde{W}(\omega) = \Theta\left(1 - \frac{|\omega|}{\epsilon}\right) \longleftrightarrow W(t) = \frac{2\,\sin(\epsilon t)}{t}, \tag{46}$$

where $\epsilon > 0$ is the cutoff frequency. With Parseval's theorem and the convolution theorem of the Fourier transform,

$$(\tilde{R} * \tilde{\phi}_{\mathrm{ML}})(\omega) \longleftrightarrow R(t)\phi_{\mathrm{ML}}(t), \tag{47}$$

we write in a first step

$$\begin{aligned}\xi_{\mathrm{ML}} &= \int_{-\infty}^{+\infty} d\omega\, \tilde{W}(\omega)(\tilde{R} * \tilde{\phi}_{\mathrm{ML}})(\omega) \\ &= \frac{1}{2\pi}\int_{-\infty}^{+\infty} dt\, W(t)R(t)\phi_{\mathrm{ML}}(t).\end{aligned}$$

Defining the auxiliary function

$$H(t) \equiv W(t)R(t)\phi_{\mathrm{ML}}(t), \tag{48}$$

and noting that all functions on the r.h.s. are even in time, it follows that

$$\xi_{ML} = \frac{1}{\pi}\int_0^{\infty} dt\, e^{-st}H(t)\Big|_{s=0}. \tag{49}$$

The pseudoelastic contribution ξ_{ML} may, thus, be written as Laplace transform of a product of three functions, evaluated at $s = 0$. We use now that for a pair of functions, $f(t)$ et $g(t)$,

$$\int_0^{\infty} dt\, e^{-st} f(t)g(t) = \frac{1}{2\pi i}\oint_C ds'\, \hat{f}(s - s')\hat{g}(s'), \tag{50}$$

where C encircles all singularities of the integrand, and use this formula in two steps:

1. Compute

$$\hat{\phi}^{(R)}_{\mathrm{ML}}(s) = \frac{1}{2\pi i}\oint_C ds'\, \hat{\phi}_{\mathrm{ML}}(s - s')\hat{R}(s'). \tag{51}$$

2. Compute

$$\xi_{ML} = \frac{1}{\pi}\left\{\frac{1}{2\pi i}\oint_C ds'\, \hat{\phi}^{(R)}_{\mathrm{ML}}(-s')\hat{W}(s')\right\}. \tag{52}$$

Here, an analytical form is known for the Laplace transformed model relaxation function, $\hat{\phi}_{\mathrm{ML}}(s)$ [see Eq. (39)], for the Laplace transform of the model resolution time window,

$$\hat{R}(s) = \frac{1}{\sigma}\sqrt{\frac{\pi}{2}}e^{\frac{s^2}{2\sigma^2}}\,\mathrm{erfc}\left(\frac{s}{\sqrt{2}\sigma}\right), \tag{53}$$

and for the Laplace transform of $W(t)$,

$$\hat{W}(s) = 2\mathrm{arccot}\left(\frac{s}{\epsilon}\right). \tag{54}$$

An analytical form of the contour integrals (51) and (52) cannot be found, but a good quasi-analytical approximation can be obtained by replacing $\hat{R}(s)$ and $\hat{W}(s)$ by Padé approximants,[33]

$$\hat{R}(s) \approx \frac{1}{\sigma}\frac{P(s/\sigma)}{Q(s/\sigma)}, \tag{55}$$

$$\hat{W}(s) \approx \frac{P'(s/\epsilon)}{Q'(s/\epsilon)}, \tag{56}$$

where $P(\cdot), Q(\cdot), P'(\cdot), Q'(\cdot)$ are polynomials. We note here that the method has been recently used to compute a good approximation for the resolution-broadened Fourier transform $\tilde{\phi}^{(R)}_{\mathrm{ML}}(\omega)$.[14] Introducing appropriately scaled integration variables, the contour integrals (51) and (52) may then be evaluated by the residue theorem of complex analysis. The details are described in the Appendix, and the result is

$$\xi_{\mathrm{ML}} \approx \frac{1}{\pi}\sum_{j=1}^{m}\sum_{k=1}^{m'}\chi\lambda c_j d_k \hat{\Phi}_{\mathrm{ML}}(-\chi(u_j + \lambda v_k)), \tag{57}$$

where $\hat{\Phi}_{\mathrm{ML}}(\cdot)$ is the scale-free version of the Laplace-transformed relaxation function $\hat{\phi}_{\mathrm{ML}}(\cdot)$,

$$\hat{\Phi}_{\mathrm{ML}}(u) = \frac{1}{u(1 + u^{-\alpha})}, \tag{58}$$

χ and λ are the dimensionless scaling parameters,

$$\chi = \sigma\tau \quad \text{and} \quad \lambda = \frac{\epsilon}{\sigma}, \tag{59}$$

and $\{u_j\}$ and $\{v_k\}$ are the roots of the polynomials $Q(u)$ and $Q'(v)$, respectively. The coefficients

$$c_j = \frac{P(u_j)}{\Pi^m_{k=1,k\neq j}(u_j - u_k)}, \tag{60}$$

$$d_k = \frac{P'(v_k)}{\Pi^{m'}_{l=1,l\neq k}(v_k - v_l)} \tag{61}$$

are the residues of the dimensionless expressions $P(u)/Q(u)$ and $P'(v)/Q'(v)$, evaluated at the respective roots of the denominator polynomials. We have, thus, $Q(u_j) = 0$ and $Q'(v_k) = 0$. The final expression (57) for ξ_{ML} is, thus, the linear superposition of simple terms of the form (58). Coding ξ_{ML} as a compiled function leads to sufficiently short execution times, which allow for integrating this function into a fitting procedure.

D. Numerical test

To obtain a systematic picture of the pseudoelastic contribution as a function of τ and α, we compute it according to Eq. (57) for $\alpha = k \times 0.1$, $k = 0, \ldots, 10$. In view of later applications, we define σ to be the resolution (HWHM) of the IN16B spectrometer, $\sigma = 1.75$ μeV, and we set $\epsilon = 3\sigma$. We vary then $\chi \in [\sigma\tau_{\min}, \sigma\tau_{\max}]$, where $\tau_{\min} = 0.1$ ps and $\tau_{\max} = 10^4$ ps (solid lines). For comparison, we compute ξ_{ML} by numerical integration of $\phi^{(R)}_{\mathrm{ML}}(\omega)$, choosing the same values for α, σ, and ϵ and fixing τ to the

Published under an exclusive license by AIP Publishing

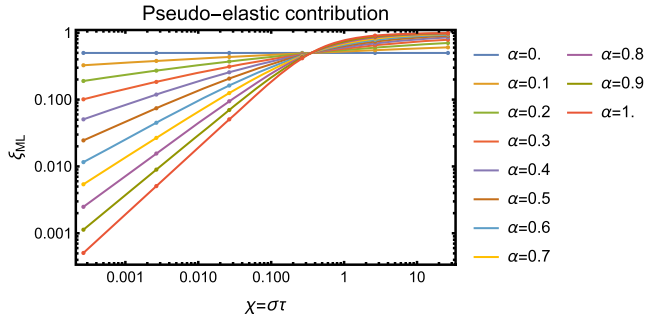

FIG. 1. Pseudoelastic contribution ξ_{ML} as a function of $\chi \equiv \sigma\tau$ and α. The solid lines correspond to the calculation according to Eq. (57) and the points to control calculations by numerical integration. More explanations are given in the text.

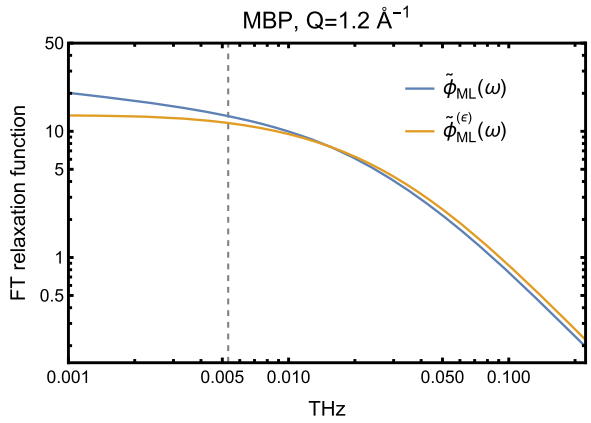

FIG. 2. Impact of global diffusion on the Fourier spectrum of the model relaxation function for MBP in D_2O buffer at T = 283 K and q = 1.2/Å. The solid blue line labels the relaxation function and the yellow line the corresponding function with the diffusion damping factor, where D = 3.3 Å^2/ns from DLS. The vertical dashed indicates the instrumental resolution (FWHM).

discrete values $\tau = 10^j$ ps, $j = -1, \ldots, 4$ (points). Defining the matrices $\boldsymbol{\xi}_{ML} \equiv (\xi_{ML}[j,k])$ and $\boldsymbol{\xi}^{(n.i.)}_{ML} \equiv (\xi^{(n.i.)}_{ML}[j,k])$, where "n.i." stands for "numerical integration," we find that

$$\|\boldsymbol{\xi}^{(n.i.)}_{ML} - \boldsymbol{\xi}_{ML}\| = 3.45 \times 10^{-6},$$

where $\|\cdots\|$ is defined as the maximum singular value of the difference matrix. The results of the calculations are shown in Fig. 1. On observes that for "good resolutions," where $\sigma\tau < 1$, the pseudoelastic contributions increase with decreasing α, and the opposite is true for "bad resolutions," where $\sigma\tau > 1$. We note that $\lim_{\alpha\to 0}\phi_{ML}(t) = 1/2$ for any $t > 0$, which explains the results for $\alpha = 0$. All calculations have been performed with Padé-approximations of order $m = 8$ for the denominator polynomials $Q(u)$ and $Q'(u)$ and order $n = 8$ for the corresponding numerator polynomials, $P(u)$ and $P'(u)$, choosing $s = 1$ as the reference point. Constructing the Padé-approximant for the resolution function through

$$\tilde{R}_{Padé}(\omega) \equiv \frac{1}{\pi}\Re\left\{\frac{P(i\omega)}{Q(i\omega)}\right\},$$

we find that

$$|\tilde{R}_{Padé}(\omega) - \tilde{R}(\omega)| < 10^{-6}$$

in the relevant ω-domain. All computations have been performed with the Wolfram Mathematica software.[34]

IV. APPLICATIONS

A. QENS analysis of Myelin Basic Protein

To illustrate the pseudoelastic contribution to elastic scattering we consider now a concrete example related to a recently published QENS study of Myelin Basic Protein (MBP) in an aqueous solution.[15] Myelin Basic Protein is an elementary constituent of the myelin sheath of nerves and in aqueous solution, it is an intrinsically disordered protein (IDP). The incoherent QENS spectra for the study cited above have been recorded on the new IN16B spectrometer of the Institut Laue-Langevin, using the BATS option (Backscattering And Time-of-flight Spectrometer) with an instrumental resolution (FWHM) of 3.5 μeV. The translational diffusion constant, D, of MBP was measured separately by dynamic light scattering (DLS) and was then injected into the fit, writing $F^{(+)}(q,t) = \exp(-Dq^2|t|)F^{(+)}_{int}(q,t)$, where $F^{(+)}_{int}(q,t)$ is the symmetrized intermediate scattering function for internal motions, the generic form of which is given by Eq. (36). The implicit assumption is here that global and internal motions are not correlated. As mentioned in Ref. 15, the resulting fits for *EISF*, α, and τ vary only a little if the diffusion constant is simply neglected. This is illustrated in Fig. 2, which shows a log–log plot of the Fourier spectrum of the fitted model relaxation function for MBP in D_2O buffer (T = 283 K, q = 1.2/Å) for the dynamical range of the instrument, together with the corresponding diffusion-broadened counterpart resulting from the damping factor $\exp(-Dq^2|t|)$ of the intermediate scattering function. We take here D = 3.3 Å^2/ns from DLS. Having this figure in mind, the resolution-deconvolved intermediate scattering function can, therefore, be fitted directly with the model (36). It is worthwhile mentioning that more sophisticated treatments of global protein motions have been developed,[35–38] but we consider that our estimation, which is exact for small q-values, is sufficient to estimate their impact.

The impact of pseudoelastic scattering on the observed elastic intensities is illustrated in Fig. 3, which shows again the Fourier spectrum of the fitted model relaxation function $\tilde{\phi}_{ML}(\omega)$ for the same parameters as in Fig. 2 (blue line), together with the model resolution function (yellow line), where the instrumental resolution (HWHM) corresponds to σ = 0.0027 THz, and the resulting resolution-broadened spectrum, $\tilde{\phi}^{(R)}_{ML}(\omega)$ (red line). The (dimensionless) area in light red is the corresponding pseudoelastic contribution, which is for this example $\xi_{ML} \approx 0.47$ with $\epsilon = 3\sigma$. The difference between the model spectrum and its resolution-broadened version should also be noticed.

An important result of the study in Ref. 15 was that the fitted EISF vanishes. This can be explained by the fact that MBP in solution is a very flexible molecule, such that $\langle \exp(i\mathbf{q}\cdot\hat{\mathbf{R}}_j)\rangle \approx 0$. In the Gaussian approximation[39,40] (in $q \equiv |\mathbf{q}|$) of the elastic amplitude one would write

Published under an exclusive license by AIP Publishing

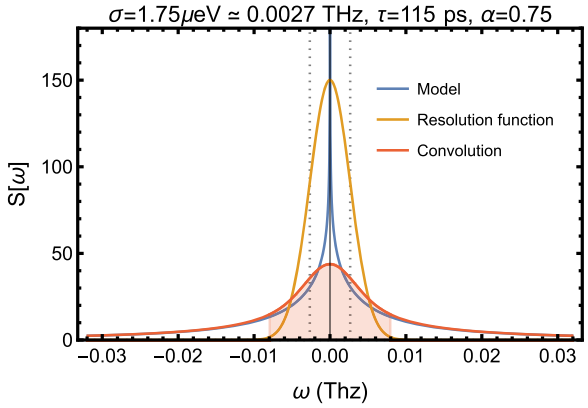

FIG. 3. Model relaxation function $\tilde{\phi}_{\mathrm{ML}}(\omega)$ (blue line), model resolution function (yellow line) and the resulting convolution $\tilde{\phi}^{(R)}_{\mathrm{ML}}(\omega)$ (red line) for the resolution of the IN16B spectrometer at ILL. The values for τ and α are taken from the fit parameters shown in Fig. 4 (three-parameter fit for $|\mathbf{q}| = 0.8/\text{Å}^{-1}$). The vertical dotted lines indicate the instrumental resolution and the light red area corresponds to the pseudoelastic contribution of $\xi_{\mathrm{ML}} \approx 0.47$ for this example.

$$EISF(\mathbf{q}) \overset{|\mathbf{q}|\to 0}{\sim} \frac{1}{N}\sum_{j\in\mathbb{H}} e^{-\frac{1}{3}|\mathbf{q}|^2\langle\hat{\mathbf{u}}_j^2\rangle} \approx 0, \tag{62}$$

where $\langle\hat{\mathbf{u}}_j^2\rangle \equiv \langle(\hat{\mathbf{R}}_j - \langle\hat{\mathbf{R}}_j\rangle)^2\rangle$ is the mean square position fluctuation of (hydrogen) atom j. For smaller q-values a vanishing EISF stands thus for large motional amplitudes of the atoms. Keeping in mind that the EISF is a "theoretical quantity," $EISF(\mathbf{q}) = F_{\mathrm{inc}}(\mathbf{q}, \infty)$, which can only be determined by assuming a model, we can now check the fits of the three-parameter model (36) with a two-parameter fit, where the EISF is eliminated according to Eq. (27). The results in Fig. 4 show that α and τ change only slightly comparing the two- and three-parameter fits, where the decrease of α with q indicates that increasingly slower relaxation modes are mixed in with decreasing spatial resolution, making the relaxation function less exponential. The vanishing EISF from the three-parameter fits is, in particular, confirmed if one considers the relevant scale for this quantity. The measured elastic intensity (bottom panel, green points) is this entirely determined by the "pseudoelastic contribution" defined in Eq. (57). For its calculation, we used the same Padé approximations as for the numerical test described in Sec. III D. We note here that the standard estimation of the parameter errors for the three-parameter fits (yellow dots) leads to error bars, which are sometimes hardly visible in the plots and cannot be performed for the two-parameter fits. The reason is purely technical—namely that in the latter case the EISF "parameter" is a compiled function, which is passed as an argument to the fit routine of the Mathematica software.[34] Concerning this point, we think that the error of the fit parameters is anyway better estimated by comparing the results of the three- and two-parameter fits.

B. QENS analysis of myoglobin

To show that the model (36) does not systematically lead to vanishing EISFs for proteins in solution, we have analyzed QENS data from apo-myoglobin at $T = 284$ K in D_2O buffer (pD = 6), which have been recorded on the IN5 spectrometer at the Institut Laue-Langevin in Grenoble, at a resolution (FWHM) of 11.6 μeV.[41] In contrast to MBP, myoglobin is a compactly folded globular protein of about the same weight, but with a well-defined three-dimensional structure containing eight α-helices as secondary structure elements. Figure 5 shows that here, as for MBP, global diffusion can be neglected for the analysis of the QENS spectra. We insert here

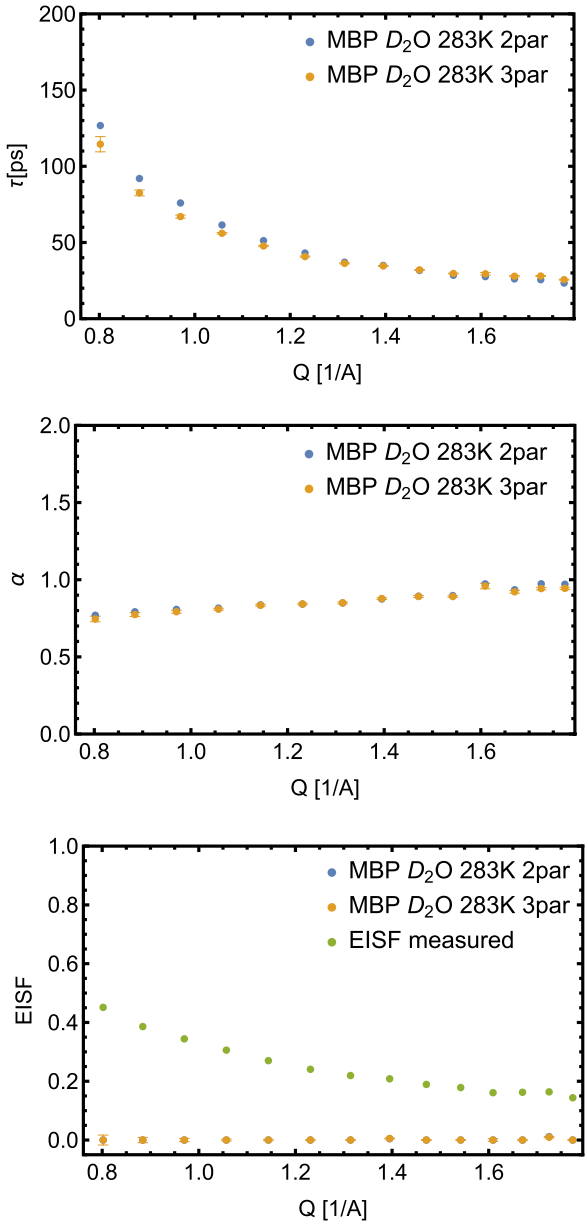

FIG. 4. From top to bottom: Characteristic time scale, τ, form parameter, α, and elastic scattering amplitude, *EISF*, for incoherent QENS from MBP in solution. Blue dots correspond to a two-parameter fit, where $EISF \equiv EISF(\tau, \alpha, \sigma)$ according to Eq. (45) and yellow points to a three-parameter fit. Concerning the EISF, the green points correspond to the measured elastic intensity $F_m(\infty) \equiv F_m(\mathbf{q}, \infty)$ defined in Eq. (25), and on the scale of the plot the results in two- and three-parameter plots are indistinguishable.

Published under an exclusive license by AIP Publishing

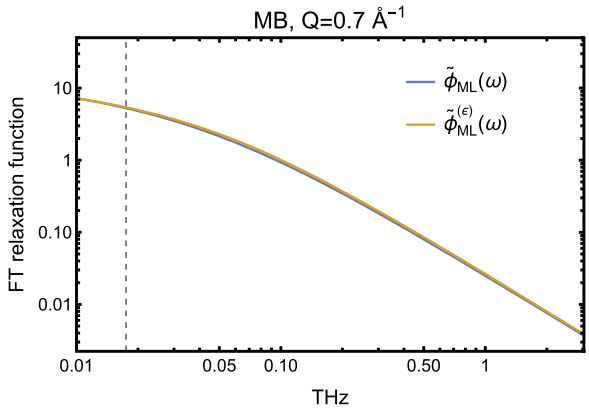

FIG. 5. Impact of global diffusion on the model dynamic structure factor at $q = 0.7$/Å for myoglobin in solution. The legends are the same as in Fig. 2.

a global diffusion coefficient of $D = 10.1$ Å^2/ns, which is the mean of the values reported in Refs. 42 and 43, respectively, but the exact value is here not important. We note in this context that a somewhat smaller value of $D \approx 8$ Å^2/ns is obtained by a very rough estimation from the Stokes-Einstein relation, $D = k_B T/6\pi\eta R_h$, inserting here a hydrodynamic radius of $R_h = 2$ nm for a myoglobin molecule and for η the kinematic viscosity of water at 284 K ($\eta = 1.306$ mPa s).[44] The hydrodynamic radius is here calculated from PDB structure 1BVC for apo-myoglobin, assuming the latter to be a sphere.

Since impact of global diffusion can be neglected, model (36) has again been fitted directly to the resolution-deconvolved intermediate scattering function. Figure 6, bottom panel, shows that the EISF for myoglobin is clearly non-vanishing and that both the three- and the two-parameter fits give again similar results. The fact that the atomic motions in a globular, compactly folded protein are more hindered than in a polymer-like intrinsically disordered protein like MBP is thus clearly reflected in the corresponding EISFs, and it should be noted that this effect is much more pronounced for the resolution-corrected elastic intensities than for the measured ones. It should also be noted that the characteristic time scale, τ, is systematically smaller compared with MBP, reflecting faster localized motions of the atoms in the more compactly folded myoglobin molecule, and that the α-values are very similar compared with MBP in the common q-interval ([0.8/Å < q < 1.06/Å]).

C. Resolution correction for $\langle \hat{\mathbf{u}}^2 \rangle$

The Gaussian approximation (62) of the EISF is also known as Debye–Waller factor and has been used for decades to analyze "elastic scans" of incoherent neutron scattering from D_2O-hydrated protein powders in the low q-region, in order to infer the average mean square position fluctuations of the (hydrogen) atoms in the protein from these data. There is a large bulk of literature on that subject and we cite here only Refs. 7, 45, and 46. It follows then from Eqs. (30) and (62) that the "true," resolution-corrected mean square position fluctuation, averaged over all atoms, is given by

$$\overline{\langle \hat{\mathbf{u}}^2 \rangle} \overset{q\to 0}{\approx} -\frac{3}{q^2} \log\left(\frac{EISF_m(q) - \xi(q)}{1 - \xi(q)} \right). \tag{63}$$

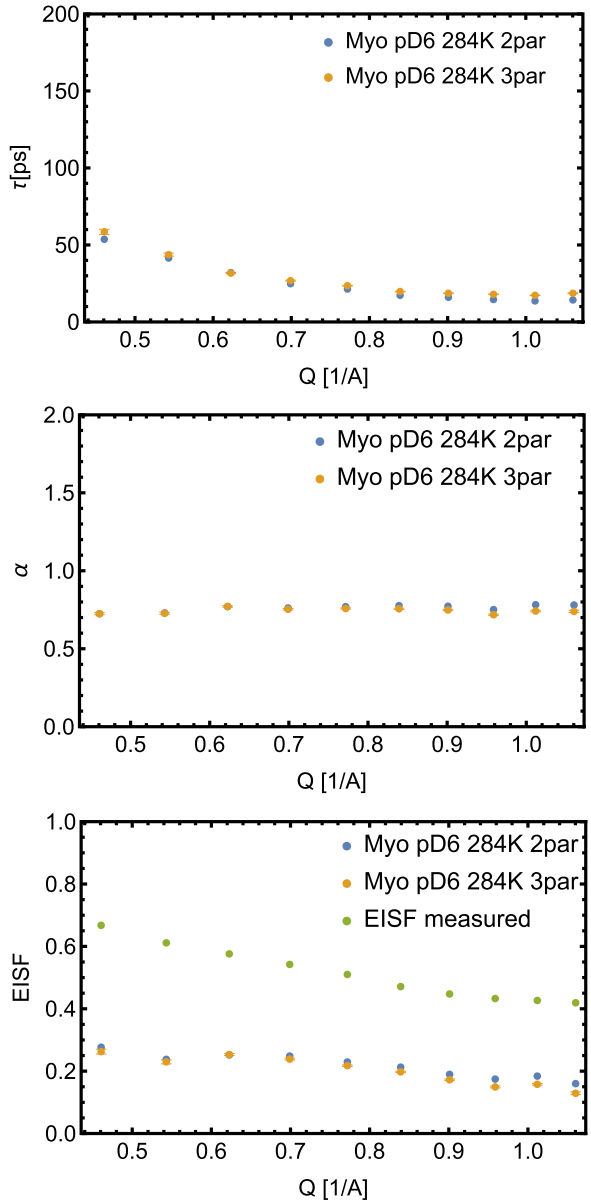

FIG. 6. The same quantities as in Fig. 6 for myoglobin in solution. More details are given in the text.

We assume here an isotropic sample and indicate explicitly the dependency of all involved quantities on $q \equiv |\mathbf{q}|$. Writing $EISF_m(q) = \exp(-q^2\overline{\langle \hat{\mathbf{u}}^2 \rangle}_m/3)$ and developing Expression (63) into a power series in $\xi(q)$, we obtain

$$\overline{\langle \hat{\mathbf{u}}^2 \rangle} \approx \overline{\langle \hat{\mathbf{u}}^2 \rangle}_m + \sum_{n=1}^{\infty} \frac{3}{nq^2} \left(e^{\frac{n}{3} q^2 \overline{\langle \hat{\mathbf{u}}^2 \rangle}_m} - 1 \right) \xi(q)^n$$
$$\overset{q\to 0}{\approx} \overline{\langle \hat{\mathbf{u}}^2 \rangle}_m \sum_{n=0}^{\infty} \xi(q)^n,$$

where the geometrical series can be summed up to give

Published under an exclusive license by AIP Publishing

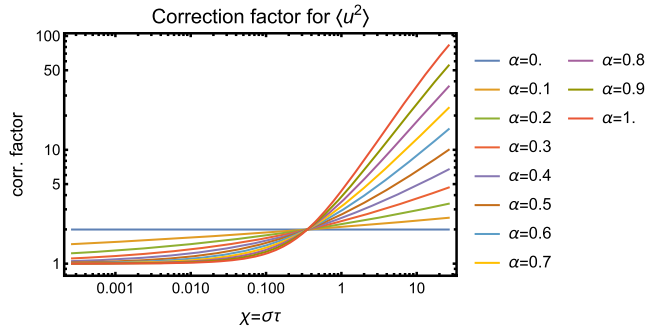

FIG. 7. Correction factor to convert the measured mean square position fluctuations into the resolution-corrected ones. More explanations are given in the text.

$$\overline{\langle \hat{\mathbf{u}}^2 \rangle} \overset{q\to 0}{\approx} \frac{\overline{\langle \hat{\mathbf{u}}^2 \rangle}_m}{1-\xi(q)}. \tag{64}$$

Figure 7 shows the correction factor $1/(1-\xi)$, which needs to be applied to obtain the "true," resolution-corrected mean square position fluctuations from the measured ones. At a first glance, the large correction factors for "bad resolutions" and close to exponential relaxation may surprise, but they can be understood noting that in this case, an elastic scan contains practically the whole integral over the quasielastic line such that $\xi \lessapprox 1$.

V. CONCLUSIONS

In this paper, we have presented a quasi-analytical method for computing the pseudoelastic contribution of quasielastic scattering to the elastic neutron scattering amplitude, which enables the estimation of the true elastic scattering amplitude for the Mittag-Leffler relaxation model. Due to the computational efficiency of the method, which is based on Padé approximants for the Laplace transformed relaxation and resolution functions, the true elastic scattering amplitude can be eliminated in the model (36) by using the measured elastic intensity and the two parameters α and τ of the ML relaxation function together with the instrument resolution, σ, as input. We have applied the method to confirm the results of a recent analysis of incoherent QENS spectra from the internal dynamics of Myelin Basic Protein in solution,[15] which revealed, in particular, a vanishing EISF. MBP is an intrinsically disordered protein and to demonstrate that the vanishing EISF is the result of its "floppiness" and the corresponding large motional amplitudes of the atoms, we performed a comparative study for myoglobin in solution. Myoglobin has about the same weight as MBP, but in contrast to the latter, it is a globular protein with a well defined structure. As one would expect, we find here a clearly non-vanishing EISF as a result of the more hindered atomic motions in a compactly folded protein. An important result in this context is that the resolution-corrected EISF shows this result much more clearly than the measured one. We have also shown that the resolution corrections of the elastic intensity may also strongly impact atomic mean square position fluctuations, which are routinely extracted from so-called elastic scans.

It should be kept in mind that the elastic intensity is a "theoretical quantity," which can only be extracted from experimental QENS spectra by assuming a model for the relaxation dynamics of the protein under consideration. In that light, our analysis is a consistency check for the ML relaxation model, which does, in principle, not exclude other models for the relaxation function.

We finally emphasize that our method is prepared to deal with a coherent scattering, in general. This aspect is, for instance, important for the increasing number of QENS studies of proteins in deuterated aqueous solutions (D_2O-buffer), where coherent scattering from the solvent becomes visible at higher momentum transfers $\gtrapprox 1.5$ Å^{-1}, if the solvent contribution is not subtracted.

ACKNOWLEDGMENTS

A.N.H. acknowledges financial support from the Région Centre-Val de Loire, France, and the Jülich Center for Neutron Science, Forschungszentrum Jülich, Germany.

AUTHOR DECLARATIONS

Conflict of Interest

The authors have no conflicts to disclose.

Author Contributions

Abir N. Hassani: Investigation (equal); Validation (lead); Visualization (lead); Writing – original draft (supporting). **Andreas M. Stadler**: Resources (lead); Writing – original draft (supporting). **Gerald R. Kneller**: Conceptualization (lead); Methodology (lead); Software (equal); Supervision (lead); Writing – original draft (equal).

DATA AVAILABILITY

The analysis code is available at https://doi.org/10.5281/zenodo.7058345 and the corresponding prepared input data for myoglobin at https://doi.org/10.5281/zenodo.7108355. The original neutron scattering data for Myelin Basic Protein are available at https://doi.ill.fr/10.5291/ILL-DATA.8-04-874.

APPENDIX: DERIVATION OF EXPRESSION (57)

We start from Eq. (51) and insert Eq. (55) for the Padé approximation of the Laplace transformed instrumental time window. In addition, we use that

$$\hat{\phi}_{\mathrm{ML}}(s) = \tau \hat{\Phi}_{\mathrm{ML}}(s\tau)$$

to obtain in a first step

$$\begin{aligned}\hat{\phi}^{(R)}_{\mathrm{ML}}(s) &= \frac{1}{2\pi i}\oint_C \frac{ds'}{\sigma}\,\hat{\phi}_{\mathrm{ML}}(s-s')\frac{P(s'/\sigma)}{Q(s'/\sigma)} \\ &\overset{s'/\sigma\to u}{=} \frac{1}{2\pi i}\oint_C du\,\tau\hat{\Phi}_{\mathrm{ML}}(\tau(s-\sigma u))\frac{P(u)}{Q(u)} \\ &= \frac{1}{\sigma}\left\{\frac{1}{2\pi i}\oint_C du\,\chi\hat{\Phi}_{\mathrm{ML}}\left(\chi\left(\frac{s}{\sigma}-u\right)\right)\frac{P(u)}{Q(u)}\right\}.\end{aligned}$$

Published under an exclusive license by AIP Publishing

Writing $Q(u) = \Pi_{k=1}^{m}(u - u_k)$ and defining the coefficients

$$c_j = \frac{P(u_j)}{\Pi_{k=1,k\neq j}^{m}(u_j - u_k)},$$

it follows then from the residue theorem of complex analysis that

$$\hat{\phi}_{\mathrm{ML}}^{(R)}(s) = \frac{1}{\sigma}\sum_{j=1}^{m}\chi c_j \hat{\Phi}\left(\chi\left(\frac{s}{\sigma} - u_j\right)\right). \tag{A1}$$

This expression is now inserted into the contour integral (52), and appropriate changes of the integration variables lead to

$$\begin{aligned}
\xi_{ML} &= \frac{1}{\pi}\left\{\frac{1}{2\pi i}\oint_C ds' \left\{\frac{1}{\sigma}\sum_{j=1}^{m}\chi c_j \hat{\Phi}\left(\chi\left(-\frac{s'}{\sigma} - u_j\right)\right)\right\}\frac{P'(s'/\epsilon)}{Q'(s'/\epsilon)}\right\},\\
&\overset{s'/\sigma\to u}{=} \frac{1}{\pi}\left\{\frac{1}{2\pi i}\oint_C du \left\{\sum_{j=1}^{m}\chi c_j \hat{\Phi}(\chi(-u - u_j))\right\}\frac{P'(u\sigma/\epsilon)}{Q'(u\sigma/\epsilon)}\right\},\\
&\overset{\epsilon/\sigma\to\lambda,u/\lambda\to v}{=} \frac{1}{\pi}\left\{\frac{1}{2\pi i}\oint_C dv \left\{\sum_{j=1}^{m}\lambda\chi c_j \hat{\Phi}(\chi(-\lambda v - u_j))\right\}\frac{P'(v)}{Q'(v)}\right\}.
\end{aligned}$$

Writing $Q'(v) = \Pi_{l=1}^{m'}(v - v_l)$ and defining the coefficients

$$d_k = \frac{P(u_k)}{\Pi_{l=1,l\neq k}^{m'}(v_k - v_l)},$$

we get again from the residue theorem the final result

$$\xi_{\mathrm{ML}} = \frac{1}{\pi}\sum_{j=1}^{m}\sum_{k=1}^{m'}\lambda\chi c_j d_k \hat{\Phi}(-\chi(u_j + \lambda v_k)), \tag{A2}$$

where $\chi \equiv \sigma\tau$ and $\lambda \equiv \epsilon/\sigma$.

REFERENCES

[1] S. Lovesey, *Theory of Neutron Scattering from Condensed Matter* (Clarendon Press, Oxford, 1984), Vol. I.
[2] *Neutron Scattering in Biology: Techniques and Applications*, Biological and Medical Physics, Biomedical Engineering, edited by J. Fitter, T. Gutberlet, and J. Katsaras (Springer, Berlin; New York, 2006), Chaps. 15 and 16, ISBN: 978-3-540-29108-4.
[3] V. G. Sakai and A. Arbe, Curr. Opin. Colloid Interface Sci. **14**, 381 (2009).
[4] J. Colmenero and A. Arbe, J. Polym. Sci., Part B: Polym. Phys. **51**, 87 (2013).
[5] R. Ashkar, H. Z. Bilheux, H. Bordallo, R. Briber, D. J. E. Callaway, X. Cheng, X.-Q. Chu, J. E. Curtis, M. Dadmun, P. Fenimore *et al.*, Acta Crystallogr., Sect. D: Struct. Biol. **74**, 1129 (2018).
[6] J. C. Smith, P. Tan, L. Petridis, and L. Hong, Annu. Rev. Biophys. **47**, 335 (2018).
[7] W. Doster, S. Cusack, and W. Petry, Nature **337**, 754 (1989).
[8] I. E. T. Iben, D. Braunstein, W. Doster, H. Frauenfelder, M. K. Hong, J. B. Johnson, S. Luck, P. Ormos, A. Schulte, P. J. Steinbach *et al.*, Phys. Rev. Lett. **62**, 1916 (1989).
[9] H. Frauenfelder, S. G. Sligar, and P. G. Wolynes, Science **254**, 1598 (1991).
[10] P. W. Fenimore, H. Frauenfelder, B. H. McMahon, and F. G. Parak, Proc. Natl. Acad. Sci. U. S. A. **99**, 16047 (2002).
[11] G. R. Kneller and V. Calandrini, J. Chem. Phys. **126**, 125107 (2007).
[12] G. R. Kneller, Proc. Natl. Acad. Sci. U. S. A. **115**, 9450 (2018).
[13] M. Saouessi, J. Peters, and G. R. Kneller, J. Chem. Phys. **150**, 161104 (2019).
[14] M. Saouessi, J. Peters, and G. R. Kneller, J. Chem. Phys. **151**, 125103 (2019).
[15] A. N. Hassani, L. Haris, M. Appel, T. Seydel, A. M. Stadler, and G. R. Kneller, J. Chem. Phys. **156**, 025102 (2022).
[16] M. H. Petersen, N. Vernet, W. P. Gates, F. J. Villacorta, S. Ohira-Kawamura, Y. Kawakita, M. Arai, G. Kneller, and H. N. Bordallo, J. Phys. Chem. C **125**, 15085 (2021).
[17] M. Bée, *Quasielastic Neutron Scattering: Principles and Applications in Solid State Chemistry, Biology and Materials Science* (Adam Hilger, Bristol, 1988).
[18] P. Gerlach, O. Schärpf, W. Prandl, and B. Dorner, J. Phys. Colloq. **43**, C7 (1982).
[19] A. M. Gaspar, S. Busch, M.-S. Appavou, W. Haeussler, R. Georgii, Y. Su, and W. Doster, Biochim. Biophys. Acta, Proteins Proteomics **1804**, 76 (2010).
[20] T. Burankova, R. Hempelmann, A. Wildes, and J. P. Embs, J. Phys. Chem. B **118**, 14452 (2014).
[21] *Neutron Scattering in Biology: Techniques and Applications*, Biological and Medical Physics, Biomedical Engineering, edited by J. Fitter, T. Gutberlet, and J. Katsaras (Springer, Berlin; New York, 2006), Chap. 15, ISBN: 978-3-540-29108-4.
[22] Q. Berrod, K. Lagrené, J. Ollivier, and J.-M. Zanotti, EPJ Web Conf. **188**, 05001 (2018).
[23] P. Schofield, Phys. Rev. Lett. **4**, 239 (1960).
[24] *Mittag-Leffler Functions, Related Topics and Applications*, Springer Monographs in Mathematics, edited by R. Gorenflo, A. A. Kilbas, F. Mainardi, and S. V. Rogosin (Springer, Heidelberg, 2014), ISBN: 978-3-662-43929-6; 978-3-662-43930-2.
[25] G. R. Kneller, Phys. Chem. Chem. Phys. **7**, 2641 (2005).
[26] G. R. Kneller and M. Saouessi, J. Phys. A: Math. Theor. **53**, 20LT01 (2020).
[27] G. R. Kneller and M. Saouessi, Acta Phys. Pol., B **53**(2), 2 (2022).
[28] W. G. Glöckle and T. F. Nonnenmacher, Biophys. J. **68**, 46 (1995).
[29] K. Oldham and J. Spanier, *The Fractional Calculus* (Academic Press, New York, London, 1974).
[30] R. Zwanzig, *Statistical Mechanics of Irreversibility*, Lectures in Theoretical Physics (Wiley-Interscience, New York, 1961), pp. 106–141.
[31] H. Mori, Prog. Theor. Phys. **33**, 423 (1965).
[32] R. Zwanzig, *Nonequilibrium Statistical Mechanics* (Oxford University Press, 2001).
[33] F. W. J. Olver, D. W. Lozier, and R. F. Boisvert, *NIST Handbook of Mathematical Functions* (Cambridge University Press, 2010), ISBN: 978-0-521-14063-8.
[34] Wolfram Research, Inc., Mathematica, Version 13.0, Champaign, IL, 2019, code available at https://doi.org/ 10.5281/zenodo.7058345 and corresponding data under https://doi.org/10.5281/zenodo.7108355).
[35] J. Pérez, J.-M. Zanotti, and D. Durand, Biophys. J. **77**, 454 (1999).
[36] A. M. Stadler, I. Digel, G. M. Artmann, J. P. Embs, G. Zaccai, and G. Büldt, Biophys. J. **95**, 5449 (2008).
[37] F. Roosen-Runge, M. Hennig, F. Zhang, R. M. J. Jacobs, M. Sztucki, H. Schober, T. Seydel, and F. Schreiber, Proc. Natl. Acad. Sci. U. S. A. **108**, 11815 (2011).
[38] M. Grimaldo, F. Roosen-Runge, F. Zhang, F. Schreiber, and T. Seydel, Q. Rev. Biophys. **52**, e7 (2019).
[39] A. Rahman, K. S. Singwi, and A. Sjölander, Phys. Rev. **126**, 986 (1962).
[40] G. R. Kneller, J. Chem. Phys. **145**, 044103 (2016).
[41] A. M. Stadler, F. Demmel, J. Ollivier, and T. Seydel, Phys. Chem. Chem. Phys. **18**, 21527 (2016).
[42] V. Riveros-Moreno and J. B. Wittenberg, J. Biol. Chem. **247**, 895 (1972).
[43] M. Rocco and O. Byron, Eur. Biophys. J. **44**, 417 (2015).
[44] M. L. Huber, R. A. Perkins, A. Laesecke, D. G. Friend, J. V. Sengers, M. J. Assael, I. N. Metaxa, E. Vogel, R. Mareš, and K. Miyagawa, J. Phys. Chem. Ref. Data **38**, 101 (2009).
[45] G. Zaccai, Science **288**, 1604 (2000).
[46] *Neutron Scattering in Biology: Techniques and Applications*, Biological and Medical Physics, Biomedical Engineering, edited by J. Fitter, T. Gutberlet, and J. Katsaras (Springer, Berlin; New York, 2006), Chap. 18, ISBN: 978-3-540-29108-4.

Published under an exclusive license by AIP Publishing